RF GUN DEVELOPMENT WITH IMPROVED PARAMETERS

V. Paramonov *, Yu. Kalinin, INR RAS, Moscow,
M. Krasilnikov, T. Scholz, F. Stephan, DESY, Zeuthen,
K. Floettmann, DESY, Hamburg

Abstract

During development and operation of DESY L-band RF gun cavities, desires for further improvements were formulated. The next step of development is based on the proven advantages of existing cavities, but includes significant changes. The L-band 1.6 cell RF gun cavity is intended for operation in pulse mode with electric fields at the cathode of up to $60\frac{MV}{m}$, RF pulse length of $\sim 1ms$ and average RF power higher than existing gun cavities. In the new design the cell shape is optimized to have the maximal surface electric field at the cathode and lower RF loss power. The cavity cells are equipped with RF probes. Cooling circuits are designed to combine cooling efficiency with operational flexibility. In the report, the main design ideas and simulation results are described.

INTRODUCTION

In the development and optimization of the high brightness electron sources for Free Electron Lasers (FELs) and linear colliders several RF gun cavities, starting from TTF Gun [1] and differing mainly in the cooling circuit design, were constructed and studied. The last results for the Gun cavities developed can be seen in [2]. Experience of operation and results of various Gun cavity parameters study are the basement of desires and ideas for further improvements. In the next step of development more significant changes are required, starting from cavity RF shape. The influence of proposed improvements on different cavity parameters should be considered and analyzed carefully.

RF CAVITY SHAPE

The profile of existing DESY 1.6 cell axial symmetrical RF Gun cavities [1] is shown in Fig. 1a together with electric field distribution. This cavity is considered further as the Reference Cavity (RC) and has the circular iris nose tip. The primary parameter of the RF Gun cavity is the RF electric field strength E_c at the photo cathode surface. The maximal electric field at the cavity surface E_{sm} in RC is at the iris tip and $E_{sm} \approx 1.2E_c$.

In the improved cavity, which is also 1.6 cell, Fig. 1b, the circular iris tip is replaced at the elliptical one. Dimensions are optimized to have $E_{sm} = E_c$. Together with E_{sm} reduction by $\sim 20\%$, the elliptical nose shape results in increasing of the coupling coefficient between cavity cells and related mode separation. The iris nose shape has no influence at the cavity quality factor Q_0 and decreases slightly $\frac{E_c}{\sqrt{W_0}}$ ratio, where W_0 is the stored energy. More RF power is necessary to get E_c required with the same Q. Cavity Q factor is increased by stronger rounding in the outer cell shapes. Different rounding combinations were considered. From practical reasons we chose the same outer radius for both cells and the same rounding radius in the first cell and in second cell near iris. The cavity operating frequency is adjusted by outer cell radius. The maximal field strength at the axis of the cells is equalized by adjusting the another radius of the second cell rounding. As the result, the cavity Q factor is increased by $\sim 10\%$ and required RF pulse power is less by $\sim 4\%$. Even taking into account effects of RF pulsed heating effects and cavity parameters change during RF pulse, [3], lower RF pulse power is required for improved cavity to get required E_c value.

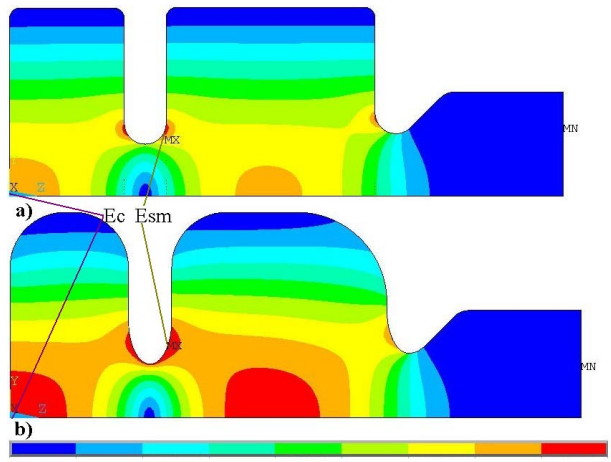

Figure 1: RF shape profile for the reference (a) and improved (f) cavity together with electric field distributions.

BEAM DYNAMIC

The cavity shape change results in small deviations of electric field distribution along the cavity and can change beam parameters. All combinations of shapes, discussed in cavity RF profile definition, were analyzed in simulations with the ASTRA code considering the European XFEL photo injector performance. Simulations revealed no essential difference for various cavity options, including RC and improved option, Fig. 1b. Optimized projected emittance for all cavity types is about the same, within simulations discrepancy. Slice parameters of the electron beam are also very similar. Optimum currents of main solenoid are within several A. Spread of optimum rms sizes of the

* paramono@inr.ru

cathode laser is within 2%. The beam dynamic requirements are not a restrictions for the proposed cavity shape changes.

PROBES

Each cavity cell has an antenna type RF probe, placed at the cavity cylindrical side. Longitudinal probe position is fixed by cavity and cooling circuit design. To minimize RF pulsed heating effect at the probe hole edges, and perturbation of azimuthal field symmetry, the probe hole radius r_h should be as small as reasonable. Sharp hole edges are not acceptable and should be rounded with a radius $r_b = r_h/2$. For $E_c = 60\frac{MV}{m}$ the expected magnetic field near the cavity wall is $\approx 92\frac{kA}{m}$, corresponding to a pulse RF loss density $P_d \approx 3.8\frac{kW}{cm^2}$ and surface temperature rise $T_s \approx 34C^o$ after $\tau = 1ms$ RF pulse. In the vicinity of the probe hole the magnetic field distribution is perturbed with local increasing up to $P_d \approx 7.5\frac{kW}{cm^2}$ and $T_s \approx 67C^o$ for $r_h = 2mm$. Hole edges rounding is required both for local P_d reduction and for smooth stress distribution. The stress values due to RF pulsed heating are proportional to T_s [3] and after $\tau = 1ms$ RF pulse the maximal stress value is estimated below yield strength of OFC copper.

To cancel the dipole component in the field perturbation and to have as lowest component a quadruple one with zero field at the cavity axis, additional holes just opposite to existing are required. It looks attractive to use additional holes for vacuum probes. But consideration of sensitivity and response time for vacuum probes connected to cavity cells through narrow hole, optimized for RF probes, have shown vacuum sensors are not useful. Additional holes are foreseen as blind.

Required probe matching can be obtained without problems for a small probe hole radius, because for $\sim 1W$ RF signal at the probe we need attenuation $\approx 67dB$.

COOLING CIRCUIT

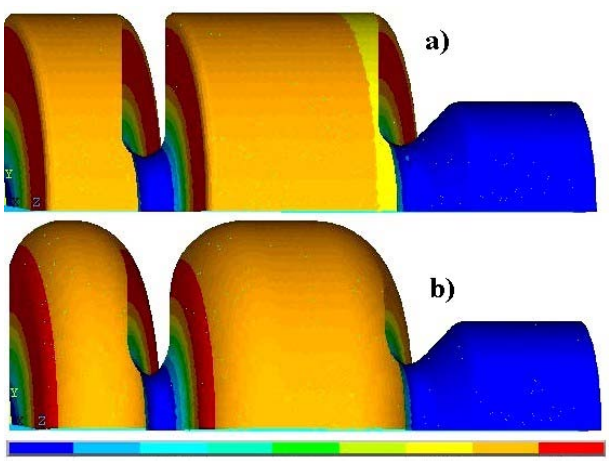

Figure 2: RF loss density distribution at the cavity surface for RC (a) and improved cavity (b). Arbitrary units.

Calculated pulse RF power values to get $E_c = 60\frac{MV}{m}$ are $P_i = 6.43MW$ for RC and $P_i = 6.18MW$ for improved cavity. For $10Hz$ repetition and $\tau = 1ms$ operation it results in average dissipated power $P_{av} \sim 65kW$ and the cavity should have an advanced cooling circuit. The distributions of RF loss density at the cavity surface are shown in Fig. 2a,b for RC and improved cavity. As one can see from Fig. 2, there is no essential qualitative difference in distributions. Cooling circuits for existing cavities are studied both in numerical simulations, see, for example [4], [5], and during cavities operation, generating ideas for improvement.

In cooling with turbulent flow a heat exchange between a cavity body and coolant takes place in a narrow boundary layer and the temperature near the center of the channel cross section is lower than near boundary. For efficient cooling we need a large amount of channels with large total surface area. The cavity surface temperature difference with respect input coolant temperature can be subdivided in three components - natural temperature drop in heat propagation from cavity surface to cooling channel surface, temperature rise in boundary layer in heat exchange with turbulent flow and bulk coolant temperature increasing in coolant motion. The distance from cavity surface to cooling channels is minimal to ensure the cavity rigid design. Large total surface area of channels is required to keep reasonable the second component. Cross section area of channels is important only to provide required flow to restrict the third component.

To have a large number of small cooling channels, we

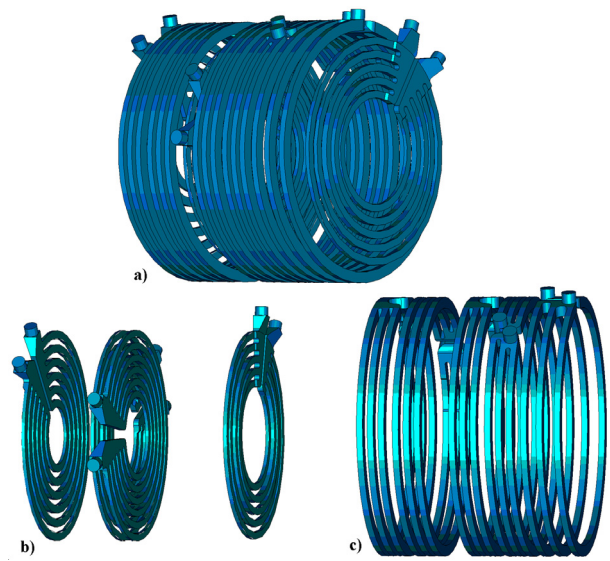

Figure 3: Proposed cooling circuit (a) consists from cooling channels for radial walls (b) and outer walls (c).

can have independent channels inside the cavity with large amount of input/output outlets and advanced distributing system outside the cavity. Proposed cooling circuit is shown in Fig. 3 and utilizes channels with flow distribution inside the cavity. The circuit has 9 cooling channels,

divided in two groups. For outer wall cooling 5 channels are proposed, Fig. 3c, with three sub channel each. These channels are equalized in hydraulic resistance and equal flow velocities in sub channels. The pressure distribution at the channel surface for RF probe region is shown in Fig. 4. Four channels for radial walls cooling, Fig. 3b, have

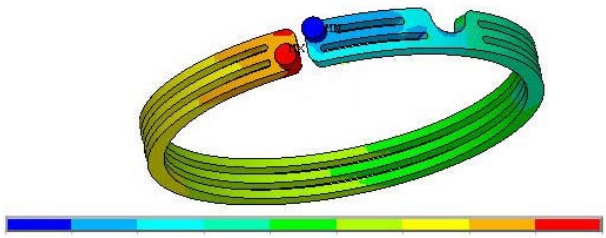

Figure 4: The pressure distribution at the surface of the channel for the RF probe region.

more complicated flow distribution. Pressure and flow velocity distributions in the channel for iris cooling are shown in Fig. 5. The flow velocities and flow rates in sub channels of channels for radial walls cooling are fitted to reflect the RF loss radial profile.

As second option for cooling channels, at least for comparison, we consider more conservative version without flow distribution within the cavity.

For cooling circuit simulations we use two approaches. In

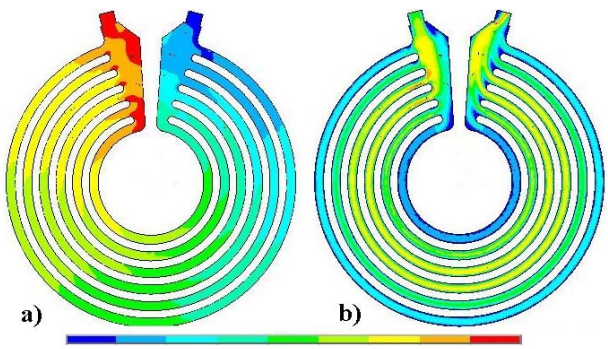

Figure 5: Pressure (a) and flow velocity (b) distributions in the channel for iris cooling.

the well known engineering approach, Fig. 6c,f, the cooling channels are considered at constant temperature and a heat exchange coefficient is defined from semi-empirical relations. In conjugated approach we specify coolant properties and pressure drop, simulate turbulent flow local parameters and solve heat exchange problem both for cavity body, Fig. 6b,e, and moving coolant flow, Fig. 6a,d. The conjugated approach provides a more logical physical picture for temperature distribution and allows to investigate in more detail particularities of flow distribution both in cooling channels itself and between connected channels, but is consuming much more in computer resources.

Comparison of calculated and measured data in DESY Gun 3 cavity have shown calculated results in temperature rise $\approx 25\%$ lower than measured. Extensive set of heat exchange experiments (hot water - cold water) has been performed to have the data for numerical model parameters calibration. This calibration now is in progress. The final results for temperature distributions in the gun cavity under development will be obtained with calibrated numerical models.

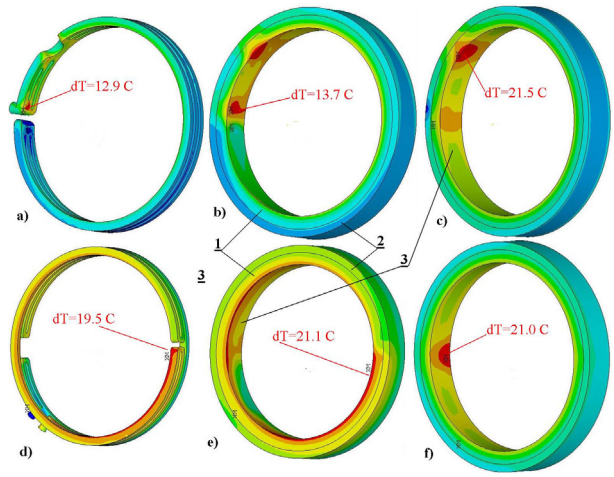

Figure 6: Temperature distributions at the surface of channels (a),(d) and at the composed ring, simulated with conjugated (b),(e) and engineering (c),(f) approaches. 1 - copper, 2 - stainless steel, 3 - surface with applied heat flux.

CAVITY DESIGN

The cavity general design is strongly based on the proven advantages of existing cavities. The cavity consist from three parts to simplify parts fabrication. Cavity has a stainless steel jacket, also segmented in three parts. It improves cavity rigidity and decreases cavity expansion in radial direction due to cavity heating. It results in decreasing of the frequency shift due to both average and pulsed RF heating. Brazing technology is foreseen to connect cavity components without water - vacuum brazed joints. The technique for iris cooling channels placement in existing cavities is applied to all channels for radial walls cooling.

REFERENCES

[1] B. Dwersteg, K. Floettmann, J. Sekutowicz, Ch. Stolzenburg. RF gun design for the TESLA VUV Free Electron Laser, NIM A 393, p.93-95, 1997.

[2] F. Stephan et al., New Experimental Results from PITZ. This Conference.

[3] V. Paramonov et al., Pulsed RF heating particularities in normal conducting L-band cavities. Proc. Linac2006, p. 646.

[4] F. Marhauser. Finite Element Analyses for RF Photoinjector Gun Cavities. TESLA FEL Report 2006-02, DESY, 2006.

[5] K. Floettmann et al., RF Gun Cavities Cooling Regime Study. TESLA-FEL Report 2008-02, DESY, 2008.